Quasi-Periodic Variability in NGC 5408 X-1

Tod E. Strohmayer[1], Richard F. Mushotzky[1], Lisa Winter[2], Roberto Soria[3], Phil Uttley[4], & Mark Cropper[5]

ABSTRACT

We report the discovery with XMM-Newton of quasiperiodic variability in the 0.2 - 10 keV X-ray flux from the ultraluminous X-ray source NGC 5408 X-1. The average power spectrum of all EPIC-pn data reveals a strong 20 mHz QPO with an average amplitude (rms) of 9%, and a coherence, $Q \equiv \nu_0/\sigma \approx 6$. In a 33 ksec time interval when the 20 mHz QPO is strongest we also find evidence for a 2nd QPO peak at 15 mHz, the first indication for a close pair of QPOs in a ULX source. Interestingly, the frequency ratio of this QPO pair is inconsistent with 3:2 at the 3σ level, but is consistent with a 4:3 ratio. A powerlaw noise component with slope near 1.5 is also present below 0.1 Hz with evidence for a break to a flatter slope at about 3 mHz. The source shows substantial broadband variability, with a total amplitude (rms) of about 30% in the 0.1 - 100 mHz frequency band, and there is strong energy dependence to the variability. The power spectrum of hard X-ray photons (> 2 keV) shows a "classic" flat-topped continuum breaking to a power law with index 1.5 - 2. Both the break and 20 mHz QPO are detected in the hard band, and the 20 mHz QPO is essentially at the break. The QPO is both strong and narrow in this band, having an amplitude (rms) of 15%, and $Q \approx 25$. The energy spectrum is well fit by three components, a "cool" disk with $kT = 0.15$ keV, a steep power law with index 2.56, and a thermal plasma at $kT = 0.87$ keV. The disk, power law, and thermal plasma components contribute 35, 60, and 5 % of the 0.3 - 10 keV flux, respectively. Both the timing and spectral properties of NGC 5408 X-1 are strikingly reminiscent of Galactic black hole systems at high inferred accretion rates, but with its characteristic frequencies (QPO and break frequencies) scaled down by a factor of 10 - 100. We discuss the implications of these findings in the context of models for ULXs, and their implications for the object's mass.

---

[1]Astrophysics Science Division, NASA's Goddard Space Flight Center, Greenbelt, MD 20771 email: stroh, richard@milkyway.gsfc.nasa.gov

[2]Astronomy Department, University of Maryland, College Park, MD 20742; lwinter@astro.umd.edu

[3]Harvard-Smithsonian Center for Astrophysics, 60 Garden St, Cambridge, MA 02138; rsoria@head.cfa.harvard.edu

[4]Astronomical Institute 'Anton Pannekoek', University of Amsterdam, Kruislaan 403, 1098 SJ, Amsterdam, the Netherlands

[5]Mullard Space Science Laboratory, University College London, Holmbury St Mary, Dorking, Surrey RH5 6NT;msc@mssl.ucl.ac.uk

Subject headings: black hole physics - galaxies: individual: NGC 5408 - stars: oscillations - X-rays: stars - X-rays: galaxies

1. Introduction

The bright X-ray sources found in nearby galaxies, the ultraluminous X-ray sources (ULX), have been the focus of considerable study over the last few years. The ULXs observed to date span a range of luminosities from several $\times 10^{39-41}$ ergs s^{-1}. To summarize, their implied isotropic luminosities may be incompatible with the Eddington luminosity of accreting black holes (BHs) whose upper mass is set by the evolution of "normal" stars (by this we mean all but the earliest populations of stars). There are basically three solutions to this luminosity conundrum; either the objects are intermediate-mass BHs (Colbert & Mushotzky 1999), or, they are stellar BHs with, in some cases, substantial beaming of their X-ray radiation (King et al. 2001); or, they are stellar-mass BHs emitting above their Eddington limit (Begelman 2006). It is possible that some ULXs appear very luminous because of a combination of all three factors (moderately higher mass, mild beaming and mild super-Eddington emission). It may also be that the ULXs are an inhomogeneous population, comprised of both a sub-sample of intermediate-mass BHs and moderately beamed stellar black holes (for recent reviews see Fabbiano & White 2006; Miller & Colbert 2004).

Efforts to unambiguously measure the masses of ULXs have been frustrated by the difficulty in finding counterparts at other wavelengths. The inability to directly detect binary motion of the putative companions has so far precluded the use of the familiar methods of dynamical astronomy to weigh these BHs (see, however, Kaaret, Simet & Lang 2006). Rather, indirect methods based on broad band spectral and timing measurements have been employed, but these are still plagued by systematic uncertainties associated with theoretical interpretation of the observed properties. For example, standard accretion disk theory predicts that at a given (fixed) value of L/L_{Edd} the inner disk temperature will scale with mass as $T \propto M^{-1/4}$ (see, for example, Frank, King & Raine 2002), thus cool thermal components (with $T < 0.5$ keV) in the spectra could be an indication of super-stellar masses. Miller and colleagues found several examples of cool disk components in the 0.1 - 0.2 keV range, most notably in the two bright ULXs in NGC 1313 (Miller et al. 2003). Comparisons with Galactic systems and the expected mass scaling give mass estimates in the $M \sim 10^{2-3}$ range. Subsequent work has found similar cool components in additional objects (Winter, Mushotzky & Reynolds 2006; Kaaret at al. 2003; Miller, Fabian & Miller 2004a; Miller, Fabian & Miller 2004b; Dewangan et al. 2004; Cropper et al. 2004; Kong, DiStefano & Yuan 2004; Stobbart, Roberts & Wilms 2006; and Feng & Kaaret 2005).

In addition to spectroscopy, X-ray timing observations of ULXs have increasingly been sought in an attempt to derive mass constraints based on comparisons with both the Galactic population of stellar BHs and the extragalactic AGNs. There is good evidence from comparison of Fourier power spectra of AGN and stellar BHs that for similar accretion states characteristic time-scales (such as power spectral break frequencies) scale with black hole mass (see, for example, Markowitz

et al. 2003). Moreover, the detailed timing properties of several stellar BHs with good mass measurements can, in principle, serve as a "calibration standard" for estimating masses of ULXs, if similar timing signatures can be detected in them. Recent successes in this area include the detection with XMM-Newton of quasi-periodic oscillations (QPOs) in the 50 - 100 mHz range from a bright ULX in M82 (Strohmayer & Mushotzky 2003; Mucciarelli et al. 2005; Fiorito & Titarchuk 2004), and subsequent detection of a break frequency (Dewangan, Titarchuk & Griffiths 2006). Although it seems likely that both the break and QPO are associated with the same ULX in M82, it has not been possible to prove this based on XMM-Newton imaging alone (see Kaaret, Simet & Lang 2006 for a discussion).

Several other ULXs have been reported to show evidence of X-ray timing signatures. Cropper et al. (2004) reported evidence for a break in the Fourier power spectrum of NGC 4559 X-7 at about 30 mHz based on XMM-Newton observations, though they also could model the spectrum with a QPO rather than a break. This source also shows evidence for a soft thermal component at 0.12 keV, similar to the "cool disk" components in other ULXs. They argued that both the spectral and timing results provide support to an intermediate-mass black hole interpretation. Soria et al. (2004) studied the ULX NGC 5408 X-1 with a series of relatively short XMM-Newton pointings. Like other ULXs, the source shows a cool thermal component ($kT \approx 0.14$ keV), but it also has a steep-spectrum radio counterpart (Kaaret et al. 2003). The radio detection has been used to argue that relativistically beamed jet emission might explain both its radio and X-ray emission. More recent radio data suggest that the radio emission is not analagous to the flat spectrum core emission seen in Galactic black holes in the low-hard state, but is more likely a radio lobe powered by jet emission from the hole (Soria et al. 2006). From the short XMM-Newton exposures it is evident that the source is quite variable, and Soria et al. (2004) reported evidence for a break in the power density spectrum at about 3 mHz. Based on the strong varibility and the need to confirm the break frequency, we proposed a longer XMM-Newton pointing at this source. In this paper we report the initial findings of these observations.

2. XMM Observations and Data Analysis

XMM-Newton observed NGC 5408 for $\approx$ 130 ksec beginning on January 5, 2006 at 19:03:57 (TT). For our study we used only the EPIC data. We used the standard SAS version 7.0.0 tools to filter and extract images and event tables for both the pn and MOS cameras. We detect the source easily and there are no source confusion problems. We extracted events in an 18" radius around the source in both the pn and MOS cameras. The observation was affected by relatively high background rates (flaring) only for relatively brief periods near the beginning and end of the pointing. We were able to produce lightcurves in three intervals of 34, 56, and 17 ksec lengths, for a total useful exposure of about 107 ksec. Figure 1 shows a combined pn+MOS lightcurve (150 s bins) including photons over the full bandpass (0.2 - 15 keV) of each instrument. The mean count rate is about 1 s^{-1}, and even by eye one can deduce that the source is varying significantly.

2.1. Power Spectral Timing Analysis

Since the countrate is higher in the pn, and it has a higher sampling rate, we began our Fourier analysis with the pn data. We broke each good interval into segments of length 16.5 ks, constructed time series sampled at 512 Hz, and calculated the power spectrum for each interval. This gave a total of 6 power spectra, each with a lower frequency bound of 6.06×10^{-5} Hz, low enough to sample the putative break frequency reported by Soria et al. (2004). The average power spectrum rebinned to 1.5 mHz resolution is shown in Figure 2. All power spectra shown here use the so called Leahy normalization, with the poisson noise level being 2 (Leahy et al. 1983). The spectrum rises below 0.1 Hz indicating the presence of significant variability, and we find a candidate QPO peak evident near 20 mHz. To further quantify the variability we fitted a model to the power spectrum. For the continuum we used a broken power-law plus a constant. While this model is adequate below about 8 mHz and above 50 mHz, it is clearly inadequate in the range between these limits. We find a statistically acceptable fit with the inclusion of three additional Lorentzian components. Fitting the power spectrum up to 0.3 Hz we find a best fit with $\chi^2 = 102.2$ for 118 degrees of freedom (dof, 132 data bins, and 14 parameters). This model fit is also shown in Figure 2 (thick solid curve). A summary of the model parameters is given in Table 1.

The strongest Lorentzian component is the QPO feature at 20 mHz. Our fit gives a centroid of 19.8 ± 0.2 mHz, a width of 3.4 ± 1 mHz, and an amplitude (rms) of $9 \pm 2\%$. If we exclude this component the χ^2 value increases by 35.1. Using the F-test to estimate the significance of the change in χ^2 associated with the 3 additional parameters for the 20 mHz QPO we find a chance probability of 1.3×10^{-7}, which is a bit better than a 5σ detection. The two other Lorentzian components are not as strongly required. We estimate F-test probabilities for the 11 mHz and 28 mHz components of 4.5×10^{-2}, and 9×10^{-4}, respectively. Based on our modeling of this spectrum alone we conclude there is good evidence for a 20 mHz QPO, with some evidence for additional variability components in the 8 - 30 mHz range. In particular the apparent need for the higher frequency component is related to the rather steep rise in the power spectrum below 40 mHz. While no sharply peaked QPO bump is evident here, the quick rise in Fourier power is significant. Whether this is truly a QPO, or part of a more complex variability continuum is difficult to say based solely on this power spectrum.

Our model fit gives a break frequency, $\nu_b = 3.5 \pm 0.4$ mHz, that appears to be consistent with that initially reported by Soria et al. (2004) based on shorter observations. To assess the need for the break in the power-law component we also modelled the power spectrum with only a single power-law but including the three Lorentzian components. This model does not fit very well, and χ^2 increases by more than 40, which is very significant based on the F-test. We therefore conclude that the break is real. The broken power-law continuum has an integrated amplitude (rms) of 15.5% in the 0.1 - 1000 mHz frequency band.

Mucciarelli et al. (2006) found that the QPO associated with a ULX in M82 could vary in frequency on timescales of hours. We separately examined the power spectra of the three individual

good time intervals to see if the 20 mHz QPO could be detected and if any time dependence was evident. The longest continuous good interval (interval 2, 56 ksec) shows a particulary strong QPO peak at 20 mHz (see Figure 3). The other good time intervals show indications of excess power at 20 mHz, but the signal to noise ratio is lower than for interval 2. We did not find any strong evidence for variation of the QPO frequency. Interestingly, in this data interval the "bump" just above 10 mHz also becomes more prominent. We fitted the same model as discussed above and found that exclusion of this Lorentzian component in the fit now increases χ^2 by 15.3. This gives an F-test probability of a little less than 1/1000 against the presence of this component in this power spectrum. Indeed, a power spectrum using only the first 33 ksec of interval 2 shows a pair of rather prominent peaks (see Figure 4). In this spectrum the statistical requirement for *both* QPO peaks is strong; the F-test yields chance probabilities of 2×10^{-7}, and 1×10^{-10} for the 14 and 20 mHz features, respectively. While the evidence for two QPOs in the average of all the data is relatively modest, it is much stronger when the more robust 20 mHz feature is also more prominent. Since we did some additional data selections when looking at the 2nd good time interval, the above probabilities should be increased by a trials penalty, but even using a factor of ten (which is conservative), we still have rather strong statistical indications for a pair of QPOs during this interval. We suggest that NGC 5408 X-1 can sometimes show a pair of sharp, closely spaced QPOs. We will have more to say about the possible implications of this shortly.

We also explored the energy dependence of the variability by creating power spectra in two broad bands, 0.2 - 2 keV, and $>$ 2 keV. In order to increase the count rates we used both the pn and MOS for this study. Figure 5 shows the average power spectrum in the hard band for all the data. A narrow feature at 20 mHz is readily apparent, and the overall power spectral shape is strikingly reminiscent of the "flat-topped" noise with a QPO and break commonly seen in many Galactic systems (see for example, McClintock & Remillard 2006). We find that this power spectrum is well fitted by a broken power-law continuum, but not a single power-law, and we derive a break frequency of 25.2 ± 5 mHz. The band limited noise component has an amplitude (rms) of 24%. Figure 6 compares the power spectra in the hard and soft bands. Interesting energy dependences are evident, with the soft flux contributing more variability power at low frequencies, with the result that the derived break frequency and the slope above the break both depend on energy. An effect like this has also been seen in Galactic BHs (Reig, Belloni & van der Klis 2003). The QPO peak at 20 mHz is remarkably sharp in this energy band, we derive a coherence, $Q \equiv \nu_0/\sigma_{lore} = 25$, and an amplitude (rms) of 15%. Comparison of this amplitude with that in the full band shows that the QPO amplitude increases with energy, a common feature of QPOs in Galactic binaries as well.

2.2. Energy Spectral Analysis

As noted in the Introduction, previous spectral studies have shown that NGC 5408 X-1 has a cool thermal component with $kT \approx 0.14$ keV (Kaaret et al. 2003; Soria et al. 2004). We obtained a

pn spectrum by extracting an 18" region around the source. Background was obtained from a nearby circular region free of sources. We first fitted a model including emission from a relativistic disk (*diskpn* in XSPEC) and a power-law. These components were modified by successive photoelectric absorption components, one fixed at the best Galactic value ($n_H = 5.7 \times 10^{20}$ cm^{-2}), the other left free to account for possible local absorption. Interestingly, this model does not provide an adequate fit, resulting in $\chi^2 = 818$ with 668 dof. The nature of the residuals suggest the possibility of thermal plasma emission, so we added an *apec* component and fitted again. Including the *apec* component results in an acceptable fit with $\chi^2 = 682.3$ for 666 dof (see Table 2 for a summary of spectral parameters, and Figure 7 for a plot of the energy spectrum and best fitting model). Such a component may be fairly common in ULXs as this is now one of several sources with such indications in its spectrum, the others being a recently found object in NGC 7424 (Soria et al. 2006), and Holmberg II X-1 (Dewangan et al. 2004). The inferred disk temperature of 0.15 ± 0.01 keV, and power-law index of 2.56 ± 0.04 are similar to earlier findings. The unabsorbed flux is 3.15×10^{-12} ergs cm^{-2} s^{-1} (0.3 - 10 keV), and implies an X-ray luminosity of 8.7×10^{39} ergs s^{-1} (at a distance of 4.8 Mpc, Karachentsev et al. 2002). The power-law, black body, and *apec* components contribute, 60.5, 34.8, and 4.6 % of the energy flux, respectively.

3. Discussion and Summary

Our XMM-Newton observations of NGC 5408 X-1 reveal a wealth of new X-ray variability phenomena. We have found strong evidence for a QPO at 20 mHz, as well as a break in the power spectral continuum near the QPO frequency. This is the 2nd ULX to show evidence for both a QPO and break in its power spectrum, the other being a ULX in M82 (Dewangan et al. 2006). In addition, during the time when the 20 mHz QPO is strongest, we also find evidence for a 2nd QPO at 14.8 mHz (see Figure 4). This is the first evidence for a pair of closely spaced QPO peaks in a ULX. Above about 2 keV the form of the power spectrum is clearly that of "flat-topped" noise breaking to a power-law with index of order 1.5 - 2, with a QPO at or near the break frequency. This form is common among Galactic black hole systems, and is most often associated with sources in either the low-hard state and/or the very high state (the steep power-law state, in the nomenclature of McClintock & Remillard 2006). The break frequency we derive appears to depend on the energy band, with the inferred break increasing with energy. This behavior is also seen in Galactic systems (see Belloni et al. 1996; Reig et al. 2003).

What do these results imply for the mass of NGC 5408 X-1? Both its X-ray spectral and timing properties are suggestive of a black hole at a relatively high mass accretion rate (relative to the Eddington rate). In terms of state definitions we would suggest that an analogy with either the very high state or perhaps the "intermediate" state is more appropriate than that of a classical low-hard state. Although low-hard state power spectra often show the "flat-topped" power continuum, QPOs are rarer than in the very high state, and the steep (energy) power-law and high luminosity of X-1 are even more problematic for a low-hard state analogy. In addition to this X-ray evidence,

the radio counterpart to X-1 has a steep spectrum that is inconsistent with the flat spectrum, compact jets seen from Galactic systems in the low-hard state.

We thus suggest that the 20 mHz QPO reported here is analogous to those identified in several Galactic systems and whose frequency is strongly correlated with parameters describing the energy spectrum, for example, the slope of the power-law component. Systems which show this behavior include XTE J1550-564 (hereafter 1550), GRO J1655-40 (hereafter 1655, Sobczak et al. 2000), GRS 1915+105 (hereafter 1915), XTE J1748-288, and 4U 1630-47 (Muno, Morgan & Remillard 1999; Vignarca et al. 2003). Vignarca et al. (2003) compile results from each of these objects, and the correlation is evident in their Figure 10. If a similar correlation holds for X-1 then one can infer an expected QPO frequency based on the measured spectral index, and deduce a simple mass scaling factor as the ratio of the predicted and observed QPO frequencies (see, for example, Dewangan et al. 2006; Titarchuk & Fiorito 2004).

Our spectral analysis of X-1 found a 90% confidence lower limit of $\Gamma = 2.48$ for the photon index of the power-law component (see Table 2). While there is a fair amount of scatter in the observed correlation it is nevertheless evident that no system with a power-law energy slope this high has a QPO frequency less than 2 Hz (see Vignarca et al. 2003). This would suggest a mass scaling of $2/0.02 > 100$ for X-1. The lowest accurately measured mass among the relevant Galactic systems is that of 1655 ($\approx 6.3 M_{\odot}$, Greene, Bailyn & Orosz 2001; Shahbaz 2003), which would suggest a lower limit to the mass of X-1 as $M_{X-1} > 630 M_{\odot}$. If we instead scale using the correlation measured for 1550, which also has a well determined mass ($\approx 10 M_{\odot}$, Orosz et al. 2002), we find that its QPO frequency is in the range 3 - 7 Hz when the power-law photon index is within the 1σ range we deduced for X-1. This gives a mass range from 1500 - 3500 $M_{\odot}$ for X-1. Interestingly, the correlation between disk temperature and QPO frequency deduced for XTE J1550-564 (Sobczak et al. 2000) gives a temperature range from $\approx 0.55 - 0.7$ keV for the same QPO frequency range (the inferred inner disk radius ranges from $\approx 30 - 125$ km, Sobczak et al. 2000). Using the mass - disk temperature scaling expected for standard accretion disks, $kT_{disk} \propto M^{-1/4}$, we find a mass range from $(0.55 \text{ keV}/0.15 \text{ keV})^4 = 1810$ to $(0.7 \text{ keV}/0.15 \text{ keV})^4 = 4740 M_{\odot}$ that overlaps substantially with the scaling deduced from the QPO frequency and power-law slope, that is, *both* the cool disk temperature and QPO frequency would appear to favor a IMBH interpretation for X-1. What about the luminosity? When 1550 shows QPOs in the 3 - 7 Hz frequency range its X-ray luminosity (2 - 20 keV) is about $2 - 3 \times 10^{38}$ $(d/6 \text{ kpc})^2$ ergs s^{-1}. Taking typical spectral parameters appropriate to 1550, and scaling into the 0.3 - 10 keV band, we obtain a luminosity over the same energy band that is a factor of ≈ 15 less than the observed luminosity of X-1 (assuming 1550 is 6 kpc distant). This is less than the mass scale factors inferred above from the QPO frequency and disk temperatures, however, we do not know *a priori* exactly what energy bands in which to compare luminosities. Put another way, we don't know accurately the bolometric corrections. Nevertheless, a rough comparison of X-ray luminosities would suggest a mass of $\approx 150 M_{\odot}$ for X-1 if it is radiating at the same Eddington ratio as 1550. This is about a factor of 10 less than the mass estimates deduced from the comparison of QPO frequencies above.

While the above arguments appear reasonable to us, it is possible that the correlation between QPO frequency and power-law index is not "universal." If this is the case, then deriving a mass scaling from the properties of the Galactic systems becomes more problematic. In particular, in order to deduce an accurate mass scaling based on observed QPO frequencies we should require that the accretion disks in both the Galactic BHs and ULXs extend to approximately the same relative radius (in terms of GM/c^2). For example, if the disk radius which dominates the observed "cool" disk component in NGC 5408 is relatively farther out than the location of the inner disk during observations of a Galactic BH with which it is being compared, then we could be overestimating the mass scale factor. Soria, Goncalves & Kuncic (2006) outline a "chilled disk" scenario for ULXs in which some fraction of their inner disk power is transferred to a corona and not radiated directly, and suggest that it might obviate the need for IMBHs in some ULXs. We will explore in detail the implications of this model for the mass of NGC 5408 X-1 in a subsequent paper.

In an attempt to be conservative we can try to identify a minimum mass for X-1 based on scaling from the lowest frequency QPOs *ever* observed from a particular Galactic source. For example, XTE J1550-564 has shown QPOs with frequencies at ≈ 0.1 Hz, although we note that the power-law index was much flatter (approaching 1.5), and the luminosity lower at such times. Scaling to this frequency would indicate a factor of 5 in mass, suggesting a minimum mass for X-1 near 50 $M_{\odot}$, still more massive than anything known in the Galaxy, but perhaps consistent with stellar evolution of low metallicity objects (Fryer & Kalogera 2001; Heger & Woosley 2002; Yungelson 2006). A source which has shown QPOs with frequencies near 20 mHz is 1915 (Morgan, Remillard & Greiner 1999). If the QPOs in X-1 are analogous to these lower frequency QPOs in 1915, then that would tend to argue against the need for a high mass. However, the properties of 1915 have been studied by several authors, and they conclude that these very low frequency QPOs appear to be associated with the oscillations from and to different emission states exhibited by the source (see Belloni et al. 2000). Moreover, 1915 does show higher frequency QPOs in both very high states and low hard states which fit into the timing and spectral correlations discussed above. Since X-1 does not show any strong evidence for similar rapid state changes, it seems more natural to us to associate the QPOs in X-1 with the > 1 Hz QPOs in 1915.

The evidence for a pair of sharp, closely spaced QPOs in X-1 is somewhat suggestive of the high frequency QPO pairs seen in Galactic systems (Remillard et al. 2002; Strohmayer 2001; McClintock & Remillard 2006). The frequencies of QPO pairs in Galactic systems seem to prefer a 3:2 ratio (Abramowicz & Kluzniak 2001; Remillard et al. 2002). When the QPO pair in X-1 is most prominent (see Figure 4) their centroids are accurately measured (see Table 1), and they are inconsistent with a 3:2 ratio at a little more than the 3σ level. They are also inconsistent with a simple harmonic relationship, but they are consistent with a 4:3 ratio. With just one example it is hard to know whether this has any important physical meaning. If X-1 is really a $\sim 1000 M_{\odot}$ black hole, then we would expect the analogs of the high frequency QPOs in Galactic systems to appear in the vicinity of 1 - 2 Hz, but we do not detect any significant variability above 0.5 Hz. The upper limit (90% confidence) to any QPO signal power with a coherence $Q \approx 10$ in the 0.5 - 2 Hz band is

$\approx 5\%$ (rms). This is greater than the typical broad energy band amplitudes found in the Galactic high frequency QPOs, but it is approaching the interesting sensitivity range. Several additional long pointings at X-1 would bring the limit near the 1% (rms) level where Galactic QPOs are often seen. Such a detection could solidify the IMBH hypothesis for NGC 5408 X-1 (see, for example, Abramowicz et al. 2004).

In summary, our XMM-Newton observations have revealed that NGC 5408 X-1 exhibits X-ray timing and spectral properties analogous to those exhibited by Galactic stellar-mass BHs in the "very high" or "steep power-law" state, but with the characteristic variability timescales (QPO and break frequencies) and disk temperature consistently scaled down. We infer a characteristic size for the X-ray emitting region ~ 100 times larger than typical inner-disk radii of Galactic BHs. If such a factor is entirely due to a higher BH mass, it implies an IMBH with $M \sim 1000 M_{\odot}$. However, a straightforward comparison of X-ray luminosities suggests a mass closer to $100 M_{\odot}$. The luminosity and timing data would be consistent with each other if the inner disk radius is also an order of magnitude larger than in Galactic BHs, in dimensionless units, as we shall discuss in a follow-up paper. While it remains conceivable that the object is a stellar-mass BH of exceptionally high mass we can think of no Galactic system that shows *all* of the properties it exhibits. Further observations should be able to determine if it shows X-ray timing and spectral correlations similar to the Galactic systems, and should enable tighter estimates on its mass.

REFERENCES

Abramowicz, M. A., Kluźniak, W., McClintock, J. E., & Remillard, R. A. 2004, ApJ, 609, L63.

Abramowicz, M. A., & Kluźniak, W. 2001, A&A, 374, L19.

Begelman, M. C. 2006, ApJ, 643, 1065.

Belloni, T., Klein-Wolt, M., Méndez, M., van der Klis, M., & van Paradijs, J. 2000, A&A, 355, 271.

Belloni, T., Mendez, M., van der Klis, M., Hasinger, G., Lewin, W. H. G., & van Paradijs, J. 1996, ApJ, 472, L107.

Colbert, E. J. M. & Mushotzky, R. F. 1999, ApJ, 519, 89.

Cropper, M., Soria, R., Mushotzky, R. F., Wu, K., Markwardt, C. B., & Pakull, M. 2004, MNRAS, 349, 39.

Dewangan, G. C., Titarchuk, L., & Griffiths, R. E. 2006, ApJ, 637, L21.

Dewangan, G. C., Miyaji, T., Griffiths, R. E., & Lehmann, I. 2004, ApJ, 608, L57.

Fabbiano, G. & White, N. E. 2006, in "Compact Stellar X-ray Sources," ed. W. H. G. Lewin, & M. van der Klis, (Cambridge University Press: Cambridge), pg. 475.

Feng, H., & Kaaret, P. 2005, ApJ, 633, 1052.

Fiorito, R., & Titarchuk, L. 2004, ApJ, 614, L113.

Frank, J., King, A. R. & Raine, D. 2002, in "Accretion Power in Astrophysics," (Cambridge University Press: Cambridge).

Fryer, C. L., & Kalogera, V. 2001, ApJ, 554, 548.

Greene, J., Bailyn, C. D., & Orosz, J. A. 2001, ApJ, 554, 1290.

Heger, A., & Woosley, S. E. 2002, ApJ, 567, 532.

Kaaret, P., Simet, M. G., & Lang, C. C. 2006, ApJ, 646, 174

Kaaret, P., Corbel, S., Prestwich, A. H., & Zezas, A. 2003, Science, 299, 365.

Kaaret, P. et al. 2001, MNRAS, 321, L29.

Karachentsev, I. D., et al. 2002, A&A, 385, 21.

King, A. R., Davies, M. B., Ward, M. J., Fabbiano, G. & Elvis, M. 2001, ApJ, 552, L109.

Kong, A. K. H., Di Stefano, R., & Yuan, F. 2004, ApJ, 617, L49.

Leahy, D. A., Darbro, W., Elsner, R. F., Weisskopf, M. C., Kahn, S., Sutherland, P. G., & Grindlay, J. E. 1983, ApJ, 266, 160.

Markowitz, A., et al. 2003, ApJ, 593, 96.

McClintock, J. E. & Remillard, R. A. 2006, in "Compact Stellar X-ray Sources," ed. W. H. G. Lewin, & M. van der Klis, (Cambridge University Press: Cambridge), pg. 157.

Miller, M. C., & Colbert, E. J. M. 2004, International Journal of Modern Physics D, 13, 1.

Miller, J. M., Fabian, A. C., & Miller, M. C. 2004a, ApJ, 614, L117.

Miller, J. M., Fabian, A. C., & Miller, M. C. 2004b, ApJ, 607, 931.

Miller, J. M., Fabbiano, G., Miller, M. C., & Fabian, A. C. 2003, ApJ, 585, L37.

Morgan, E. H., Remillard, R. A. & Greiner, J. 1997, ApJ, 482, 993.

Mucciarelli, P., Casella, P., Belloni, T., Zampieri, L., & Ranalli, P. 2006, MNRAS, 365, 1123.

Muno, M. P., Morgan, E. H. & Remillard, R. A. 1999, ApJ, 527, 321.

Orosz, J. A., et al. 2002, ApJ, 568, 845.

Reig, P., Belloni, T., & van der Klis, M. 2003, A&A, 412, 229.

Remillard, R, A., Muno, M. P., McClintock, J. E. & Orosz, J. A. 2002, ApJ, 580, 1030.

Remillard, R. A., Morgan, E. H., McClintock, J. E., Bailyn, C. D. & Orosz, J. A. 1999, ApJ, 522, 397.

Shahbaz, T. 2003, MNRAS, 339, 1031.

Sobczak, G. J., McClintock, J. E., Remillard, R. A., Cui, W., Levine, A. M., Morgan, E. H., Orosz, J. A., & Bailyn, C. D. 2000, ApJ, 531, 537.

Soria, R., Goncalves, A. C., & Kuncic, Z. 2006, IAU Symposium, 238, 162.

Soria, R., Kuncic, Z., Broderick, J. W., & Ryder, S. D. 2006, MNRAS, 370, 1666.

Soria, R., Fender, R. P., Hannikainen, D. C., Read, A. M., & Stevens, I. R. 2006, MNRAS, 368, 1527.

Soria, R., Motch, C., Read, A. M., & Stevens, I. R. 2004, A&A, 423, 955.

Stobbart, A.-M., Roberts, T. P., & Wilms, J. 2006, MNRAS, 368, 397.

Strohmayer, T. E., & Mushotzky, R. F. 2003, ApJ, 586, L61.

Strohmayer, T. E. 2001, ApJ, 552, L49.

Titarchuk, L., & Fiorito, R. 2004, ApJ, 612, 988.

Vignarca, F., Migliari, S., Belloni, T., Psaltis, D., & van der Klis, M. 2003, A&A, 397, 729.

Winter, L. M., Mushotzky, R. F., & Reynolds, C. S. 2006, ApJ, 649, 730

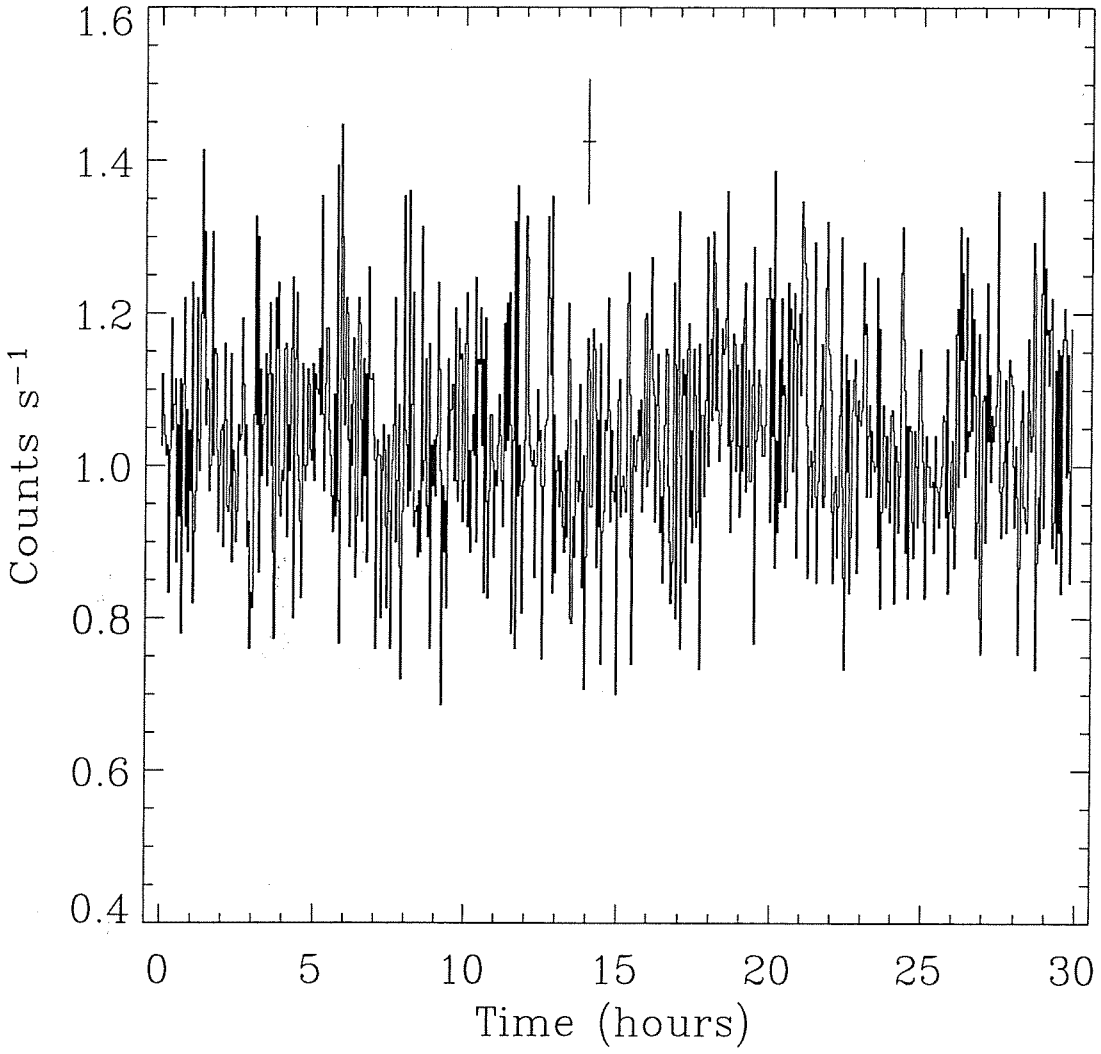

Figure 1: Lightcurve of NGC 5408 X-1 (0.2 - 15 keV band) from XMM-Newton EPIC observations. The count rate shown is the sum of the pn and MOS cameras. The bin size is 150 seconds. Time zero corresponds to MJD 53748.8378092 (TT). A characteristic error bar is also shown.

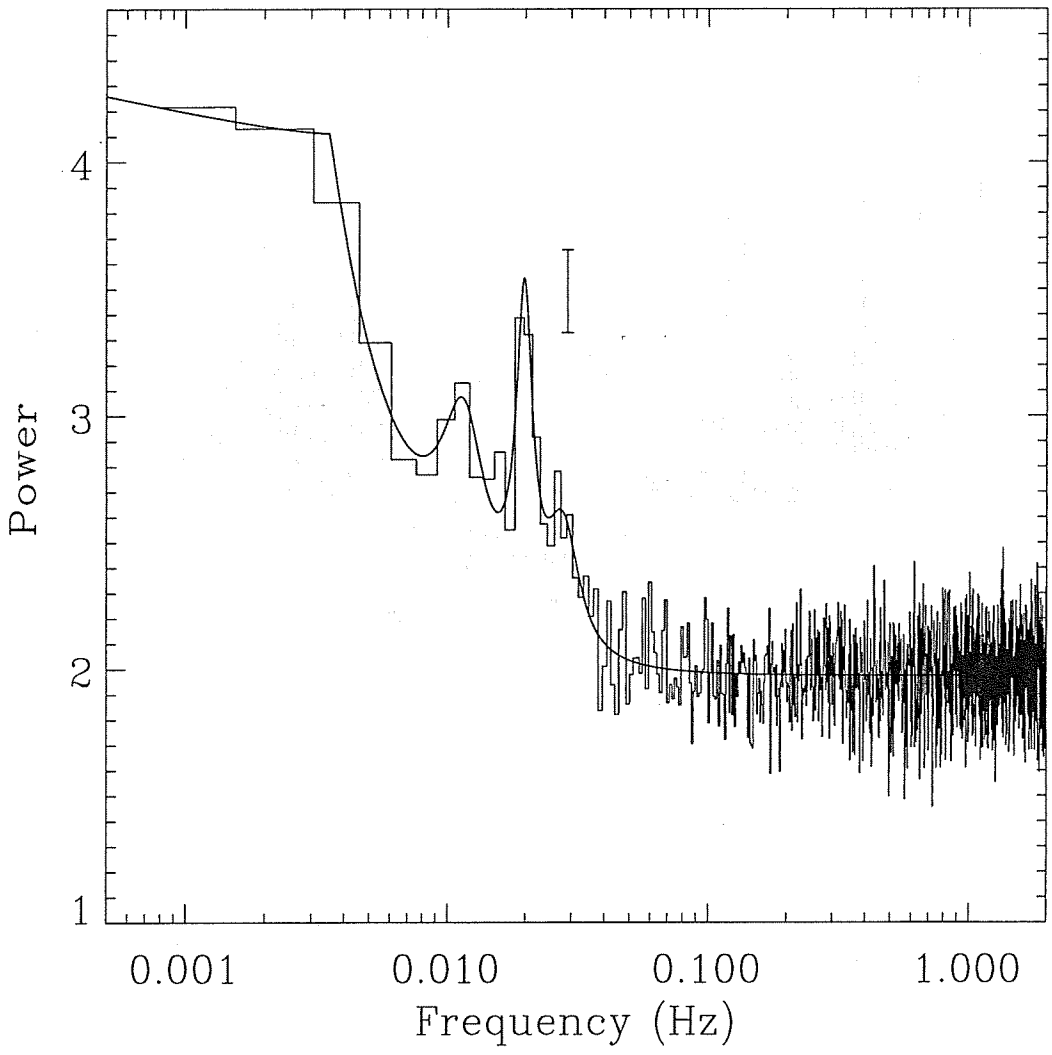

Figure 2: Average power spectrum of NGC 5408 X-1 from all the EPIC/pn data (histogram) and the best fitting model (solid). The frequency resolution is 1.52 mHz, and each bin is an average of 150 independent power spectral measurements. The effective exposure is $\approx$ 100 ksec. A characteristic error bar is also shown. See the text for a detailed discussion of the model, and Table 1 for model parameters.

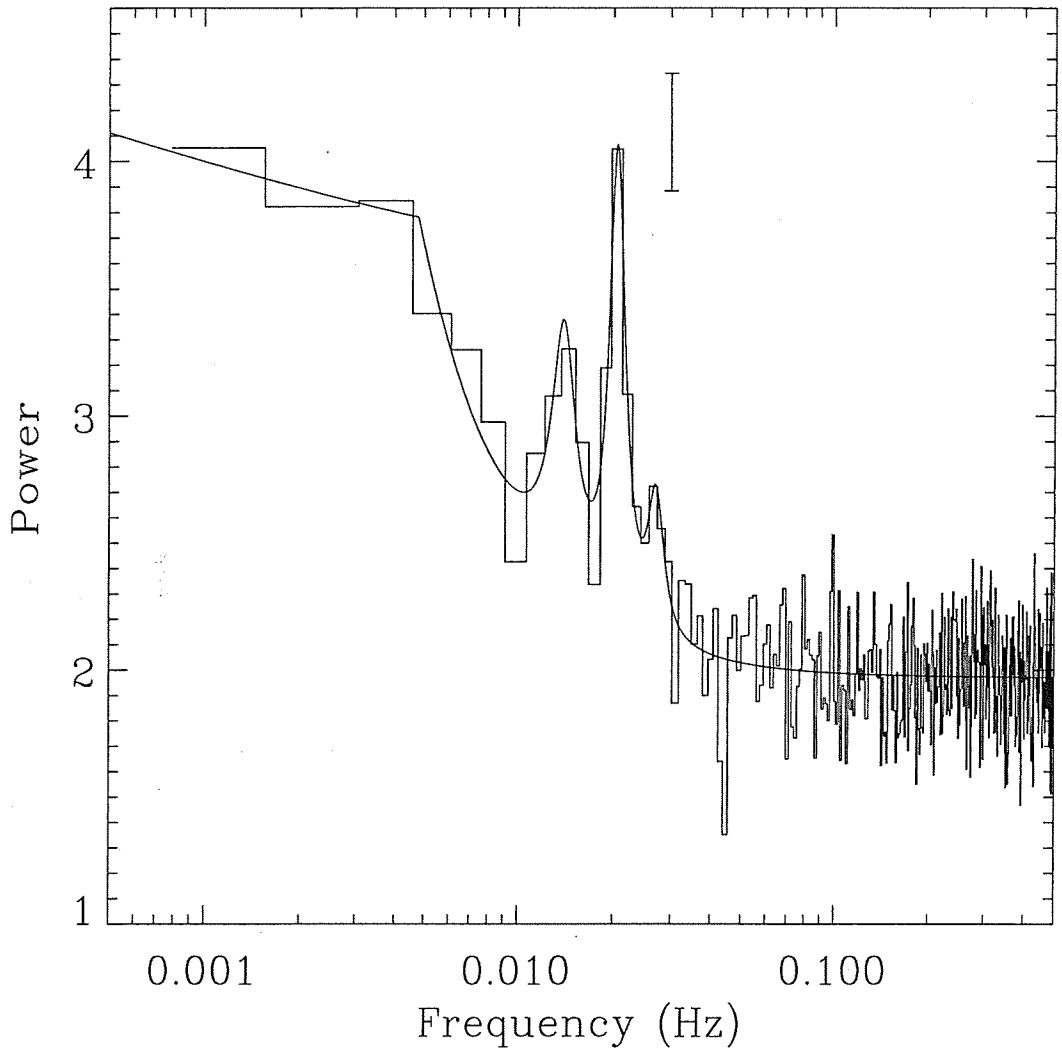

Figure 3: Average power spectrum of NGC 5408 X-1 from EPIC/pn data (histogram) and the best fitting model (solid). Here we used data only from the longest continuous good time interval ($\approx$ 57 ksec). The frequency resolution is 1.52 mHz, and each bin is an average of 75 independent power spectral measurements. A characteristic error bar is also shown. See the text for a detailed discussion of the model, and Table 1 for model parameters.

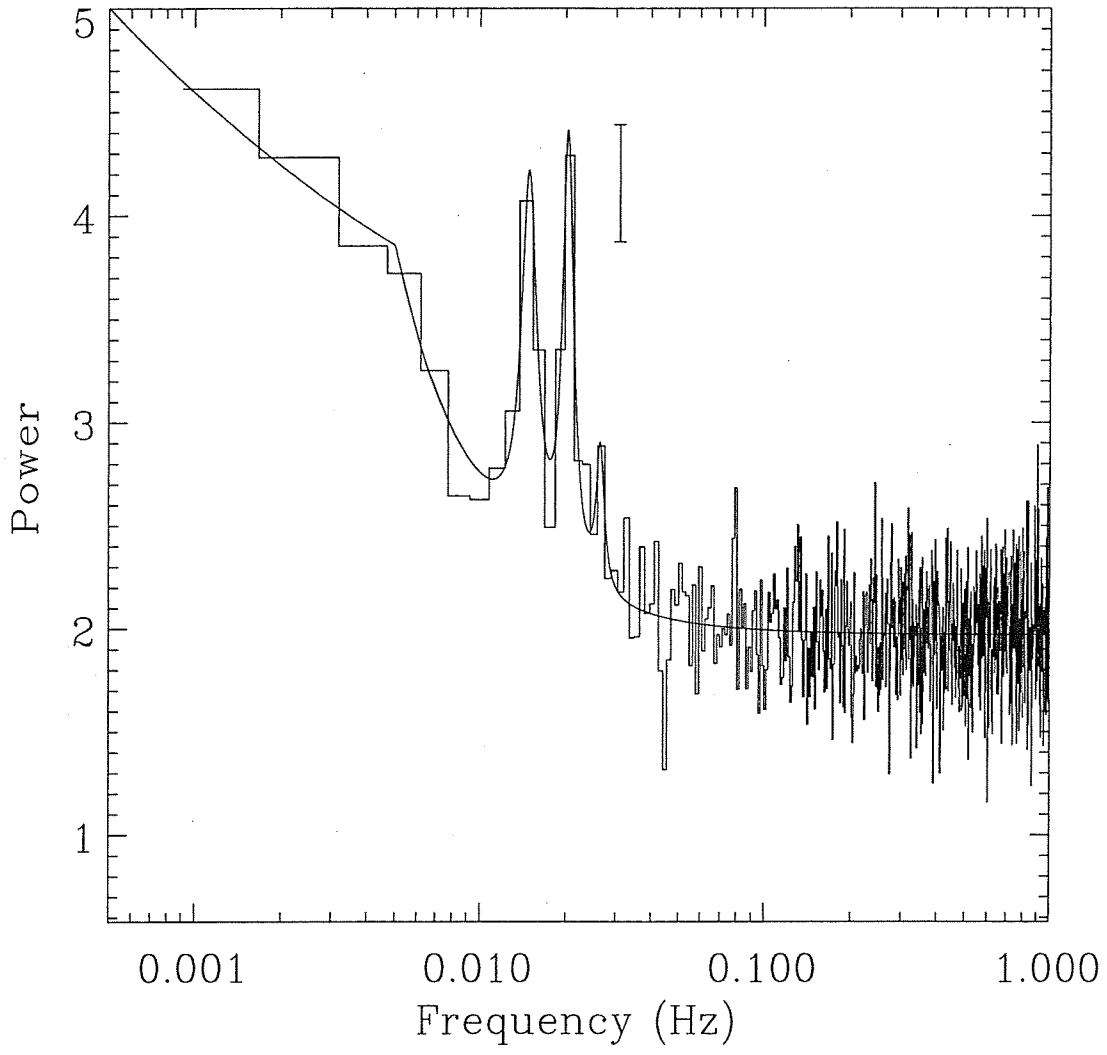

Figure 4: Average power spectrum of NGC 5408 X-1 from EPIC/pn data (histogram) and the best fitting model (solid). This spectrum was constructed from the first 33 ksec of the longest continuous time interval (interval 2). The frequency resolution is 1.52 mHz, and each bin is an average of 50 independent power spectral measurements. A characteristic error bar is also shown. See the text for a detailed discussion of the model, and Table 1 for model parameters.

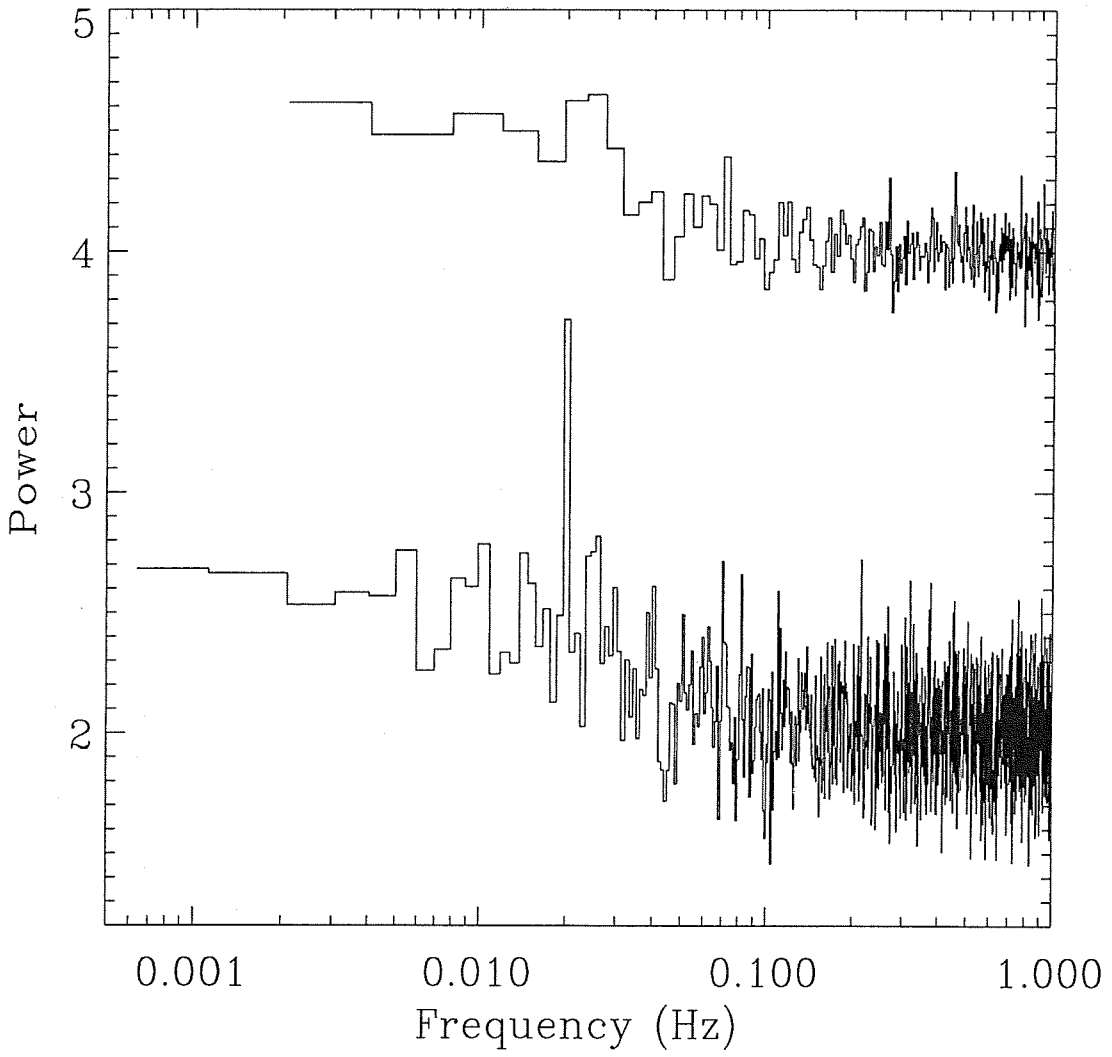

Figure 5: Average power spectrum of NGC 5408 X-1 from all EPIC/pn+MOS data. Here we used only photons with energy > 2 keV. The bottom and top curves show the same data but rebinned to different frequency resolutions of 0.97 and 3.88 mHz, respectively.

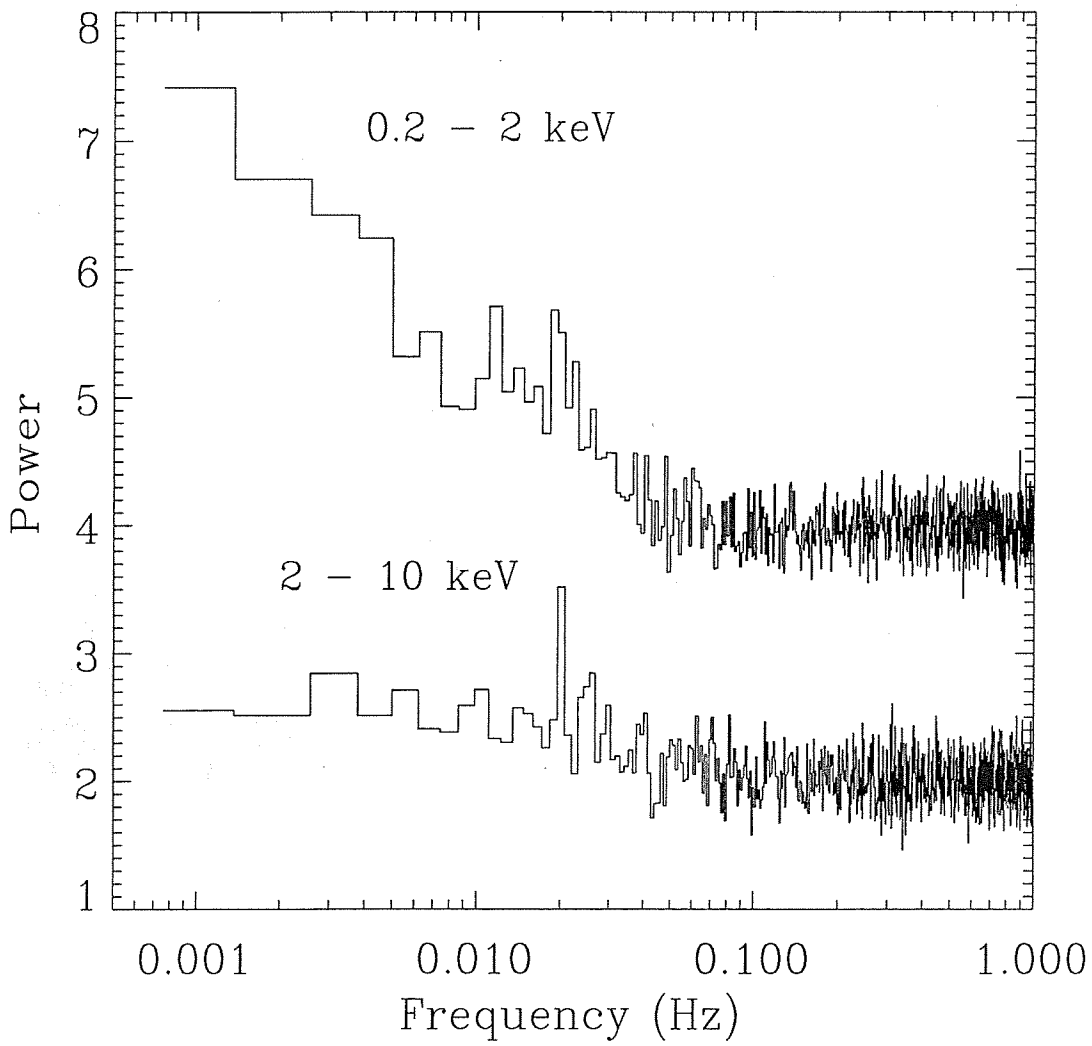

Figure 6: Comparison of average power spectra of NGC 5408 X-1 in two energy bands from EPIC/pn+MOS data. The frequency resolution is 1.2 mHz in both spectra. The upper curve is displaced vertically by 2 for clarity.

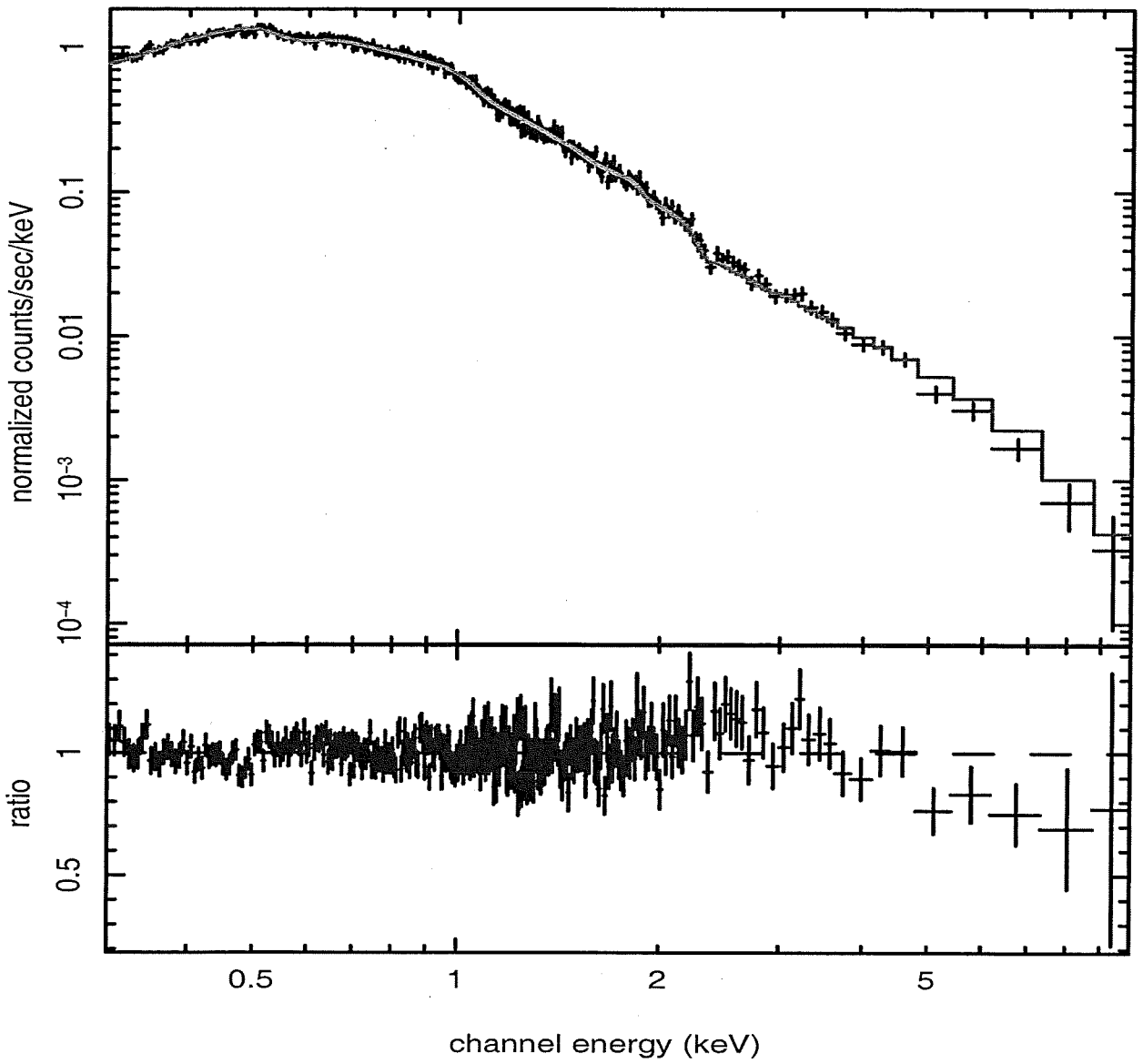

Figure 7: Energy spectrum of NGC 5408 X-1 from EPIC/pn data. The top panel shows the count rate spectrum (data points with error bars) and the best fitting model (solid histogram). The bottom panel shows the ratio of data to model. See Table 2 for details of the spectral model.

Table 1. Results of Power Spectral Modeling for NGC 5408 X-1[1]

Parameters	All pn (Fig. 2)	pn, I2 (Fig. 3)	pn, 33 ksec, I2 (Fig. 4)	All pn+MOS > 2keV
A[a]	1.57 ± 0.7	1.2 ± 0.6	0.6 ± 0.3	0.3 ± 0.1
α_1[b]	0.046 ± 0.1	0.08 ± 0.1	0.2 ± 0.1	0.13 ± 0.06
α_2[c]	1.6 ± 0.3	1.5 ± 0.4	1.4 ± 0.4	1.55 ± 0.4
$\nu_{\rm break}$ (mHz)[d]	3.5 ± 0.3	4.8 ± 0.6	4.6 ± 0.8	25.2 ± 4.5
N_1[e]	0.7 ± 0.2	0.97 ± 0.3	1.65 ± 0.7	NA
ν_1 (mHz)[f]	11.4 ± 0.7	13.9 ± 0.5	14.9 ± 0.4	NA
σ_1 (mHz)[g]	5.4 ± 2.5	3.0 ± 1.7	2.0 ± 1.0	NA
N_2	1.23 ± 0.2	1.81 ± 0.2	1.99 ± 0.4	2.1
ν_2 (mHz)	19.8 ± 0.2	20.5 ± 0.3	20.2 ± 0.3	20.5
σ_2 (mHz)	3.4 ± 1.3	2.7 ± 0.6	2.4 ± 0.7	0.4
N_3	0.5 ± 0.15	0.57 ± 0.2	0.82 ± 0.5	NA
ν_3 (mHz)	27.7 ± 2.0	27.0 ± 0.8	26.2 ± 0.9	NA
σ_3 (mHz)	10.4 ± 4.5	3.0 ± 2.0	2.0 ± 1.5	NA
χ^2 (dof)	102.2 (118)	105.1 (118)	97.0 (118)	152.2 (160)

[1]Summary of best fit power spectral models for NGC 5408 X-1. The results from fits to four different power spectra are shown in columns 2-5. Columns 2-4 show results using pn data over the full energy band, but for different time intervals. The particular time interval used is given with a reference in the heading to the figure the power spectrum appears in. These fits used three Lorentzian components, numbered 1-3 in order of increasing frequency. The last column shows results from a sum of pn and MOS data for > 2 keV photons, and only one Lorentzian component was used (at 20 mHz).

[a]Normalization of the broken power law component.

[b]Power law index below the break frequency.

[c]Power law index above the break frequency.

[d]Break frequency, in mHz.

[e]Normalization of the lowest frequency QPO component.

[f]Centroid frequency, in mHz, of the lowest frequency QPO component.

[g]Width, in mHz, of the lowest frequency QPO component.

Table 2. Spectral Fits to XMM-Newton pn Spectrum*

Spectral parameters	
Model: `tbabs*(diskpn + pow)`	
n_H[a]	$6.5^{+0.04}_{-0.10}$
T_{max}[b]	$0.176^{+0.013}_{-0.004}$
Γ	$2.56^{+0.05}_{-0.08}$
χ^2/dof	818.1/668
F_X (0.3-10 keV)[c]	3.02×10^{-12}
Model: `tbabs*(diskpn + apec + pow)`	
n_H[a]	$7.0^{+0.08}_{-0.06}$
T_{max}[b]	$0.147^{+0.014}_{-0.01}$
kT[d]	$0.873^{+0.06}_{-0.05}$
Γ	$2.56^{+0.03}_{-0.05}$
χ^2/dof	682.3/666
F_X (0.3-10 keV)[c]	3.15×10^{-12}

[a]Hydrogen column density in units of $10^{20}\,cm^{-2}$, not including the Galactic contribution of $n_{HGal} = 5.73 \times 10^{20}\,cm^{-2}$.

[b]Disk temperature in keV from the XSPEC disk model `diskpn`. The inner disk radius was fixed at $6\,GM/c^2$.

[c]Unabsorbed flux in units of $erg\,cm^{-2}\,s^{-1}$.

[d]Plasma temperature in keV from the XSPEC model `apec`. The abundances were fixed to the solar values.

*All errors are quoted at the 90% confidence level.